Collapses and explosions in self-gravitating systems

I. Ispolatov[1] and M. Karttunen[2]
[1]*Departamento de Fisica, Universidad de Santiago de Chile, Casilla 302, Correo 2, Santiago, Chile*
[2]*Biophysics and Statistical Mechanics Group, Laboratory of Computational Engineering, Helsinki University of Technology, P.O. Box 9203, FIN-02015 HUT, Finland*
(Received 3 March 2003; published 19 September 2003)

Collapse and explosion (reverse to collapse) transitions in self-gravitating systems are studied by molecular dynamics simulations. A microcanonical ensemble of point particles confined to a spherical box is considered. The particles interact via an attractive soft Coulomb potential. It is observed that a collapse indeed takes place when the energy of the uniform state is set near or below the metastability-instability threshold (collapse energy) as predicted by the mean-field theory. Similarly, an explosion occurs when the energy of the core-halo state is increased above the explosion energy, where according to the mean-field predictions the core-halo state becomes unstable. For systems consisting of 125–500 particles, the collapse takes about 10^5 single-particle crossing times to complete, while a typical explosion is by an order of magnitude faster. A finite lifetime of metastable states is observed. It is also found that the mean-field description of the uniform and core-halo states is exact within the statistical uncertainty of the molecular dynamics data.

DOI: 10.1103/PhysRevE.68.036117 PACS number(s): 64.60.−i, 02.30.Rz, 04.40.−b, 05.70.Fh

I. INTRODUCTION

Systems of particles interacting via a potential with attractive nonintegrable large r asymptotics, $U(r)\sim -r^{-\alpha}$, $0<\alpha<3$, and sufficiently short-range small r regularization exhibit gravitational phase transition between a relatively uniform high-energy state and a low-energy state with a core-halo structure [1–12]. Extensive mean-field (MF) studies of the equilibrium properties [1–11] have revealed that in a microcanonical ensemble during such a transition entropy has to undergo a discontinuous jump from a state that just ceases to be a local entropy maximum to a state with the same energy but different temperature. This state is the one with the maximum global entropy. Due to the long-range nature of gravitational interaction, the MF studies are believed to provide asymptotically (in the infinite system limit) exact information about the density and velocity distributions and other thermodynamic parameters of the uniform state. The applicability of the MF theory to the core-halo state is less obvious as the properties of the core are controlled by the short-range asymptotics of the potential.

Relatively little is known about how such a transition actually occurs, however. Youngkins and Miller [4] performed a molecular dynamics (MD) study of a one-dimensional system consisting of concentric spherical shells. Their main emphasis was to check the MF description of the stable and metastable states rather than to study the dynamics of the phase transition itself. Cerruti-Sola, Cipriani, and Pettini [12] studied the phase diagram of a more realistic three-dimensional particle system by using Monte Carlo and MD methods. Their studies again focused on the equilibrium properties of the system rather than on the dynamics of the transitions. In addition, their general conclusions about the second order of the gravitational phase transition apparently contradict the MF results [2,5,6,9]. Here, we attempt to resolve this contradiction.

A MF description of the dynamics of collapse in ensembles of self-gravitating Brownian particles with a bare $1/r$ interaction based on a Smoluchowski equation was developed by Chavanis *et al.* [8]. Their theory predicts a self-similar evolution of the central part of the density distribution to a finite-time singularity. The application of the overdamped limit used to obtain the Smoluchowski equation makes their approach essentially a tractable model of gravitational collapses with interesting properties rather than a MF description of stellar encounters. The precise nature of the random force and friction terms in the corresponding Fokker-Plank equation are not entirely understood, however.

A more rigorous approach based on the Fokker-Plank equation with the Landau collision integral was used by Lancellotti and Kiessling [13] to prove a scaling property of the central part of the density profile of a collapsing system. The model considered by them, however, allows the particles to escape to infinity, and therefore it does not have an equilibrium or even a metastable state.

There exists a vast amount of literature on cosmologically and astrophysically motivated studies of the temporal evolution of naturally occurring self-gravitating systems (see, e.g., Ref. [14] and references therein). The selection of systems and their initial and final conditions is typically astrophysically motivated; the considered systems are often too complex for making general conclusions about phase diagrams and phase transitions in such systems.

In this paper we present MD studies of gravitational collapse, and reverse to collapse, i.e., explosion, transitions in a microcanonical ensemble of self-attracting particles. Besides their pure statistical mechanical implications, these studies represent our attempt to bridge the gap between the usually complicated MD and hydrodynamic simulations of the realistic astrophysical systems and the MF analysis of the phase diagram of simple self-gravitating models.

A system with soft Coulomb potential $-(r^2+r_0^2)^{-1/2}$, where r_0 is the soft core radius, is considered. Such systems have been studied using both MF theory (see, e.g., Refs. [5,9]) and simulations [12]. We chose the microcanonical ensemble as it is the most fundamental one for the long-

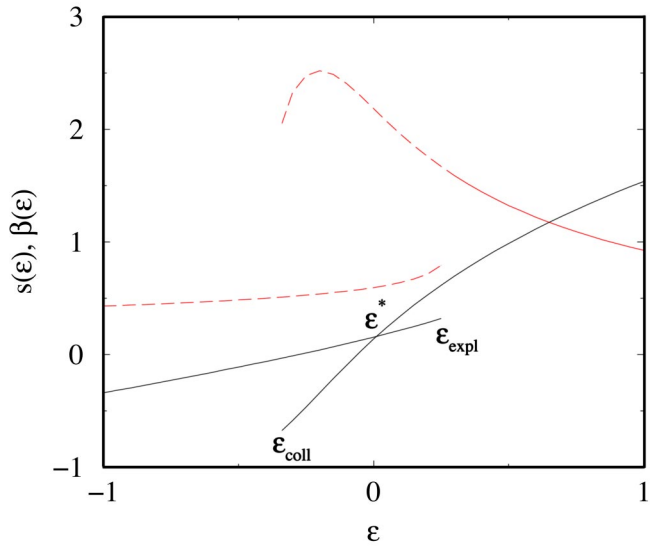

FIG. 1. Plots of entropy $s(\epsilon)$ (solid line) and inverse temperature $\beta(\epsilon)=ds/d\epsilon$ (dashed line) vs energy ϵ for a system with a gravitational phase transition and a short-range cutoff.

range interacting systems. It has to be noted that the considered system is strongly ensemble dependent: While the nature of the uniform state is the same in both microcanonical and canonical ensembles (apart from the difference in their stability range due to existence of the canonically unstable interval with negative specific heat), the core-halo states and the collapse in these ensembles have very little in common with each other [6,8].

A MF phase diagram of the system is presented in Fig. 1 [5,9]. High- and low-energy branches terminating at the energies ϵ_{coll} and ϵ_{expl} correspond to the uniform and core-halo states. The energy ϵ^*, at which the entropies of the core-halo and uniform states are equal, is the energy of the true phase transition. The uniform and the core-halo states are metastable in the energy intervals $(\epsilon_{coll},\epsilon^*)$ and $(\epsilon^*,\epsilon_{expl})$, respectively. However, for the phase transition to occur at or near ϵ^*, fluctuations at macroscopic length scales with prohibitively low entropy are required. Consequently, the metastable branches are stable everywhere except in the vicinity $\Delta\epsilon\sim N^{-2/3}$ of their end points ϵ_{coll} and ϵ_{expl} [9,15]. Here N is the number of particles in the system. Hence, it is natural to assume that once the energy of the system in the uniform state is set sufficiently near ϵ_{coll}, the system will undergo a collapse to a core-halo state with the same energy and higher entropy. Similarly, if the energy of the core-halo system is set sufficiently near ϵ_{expl}, the system will undergo an explosion bringing it to a uniform state with the same energy and higher entropy. Our goal here is to study if and how such collapses and explosions proceed in realistic three-dimensional N-particle dynamical systems.

This paper is organized as follows. In the following section we formally introduce the system, outline the MF analysis, and describe the MD setup. Then, we present the simulation results for the equilibrium uniform and core-halo states, and compare them to the MF predictions. After that, we describe and interpret the observed dynamics of the collapse and explosion transitions. A discussion concludes the paper.

II. SIMULATIONS

We consider a system consisting of N identical particles of unit mass confined to a spherical container of radius R with reflecting walls. The Hamiltonian of the system reads

$$H=\sum_{i=1}^{N}\frac{p_i^2}{2}-\sum_{i<j}^{N}\frac{1}{\sqrt{r_{ij}^2+r_0^2}}. \tag{1}$$

Using the traditional convention for self-gravitating systems (see, for example, Ref. [1]) in which the equilibrium properties of such systems become universal, we define rescaled energy ϵ, inverse temperature β, distance x, velocity u, and time τ as

$$\epsilon\equiv E\frac{R}{N^2},$$

$$x\equiv\frac{r}{R},$$

$$\beta\equiv\frac{N}{RT},$$

$$u\equiv v\sqrt{\frac{R}{N}},$$

$$\tau\equiv t\frac{N^{1/2}}{R^{3/2}}. \tag{2}$$

The unit of time, often referred to as the crossing time, $[t]=R^{3/2}/N^{1/2}$, is obtained by dividing the unit of length R by the unit of velocity $\sqrt{N/R}$. This unit of time is also proportional to the period of plasma oscillations in a medium with charge concentration N/R^3. As this time unit has purely kinematic origin, we do not expect the evolution of systems having different N and R to be universal in time τ. The evolution, assuming that it is collisional, is expected to be universal in the relaxation time $\tau_r=\tau\ln N/N$ [16], where the factor $N/\ln N$ is proportional to the number of crossings a typical particle needs in order to change its velocity by a factor of 2 through weak Coulomb scattering events.

The soft core radius $x_0=r_0/R=5\times10^{-3}$ is chosen to be well below the critical value $x_{gr}\approx0.021$, above which the collapse-explosion transition is replaced by a normal first-order phase transition [9].

The MF theory of these systems is described in detail in Ref. [5]. The equilibrium velocity distribution is Maxwellian and isothermal, while the equilibrium (saddle point) density profile $\rho(x)$ corresponding to a stable or a metastable state is a spherically symmetric solution of the following integral equation:

$$\rho(\mathbf{x})=\rho_0 F[\rho(.),\mathbf{x}],$$

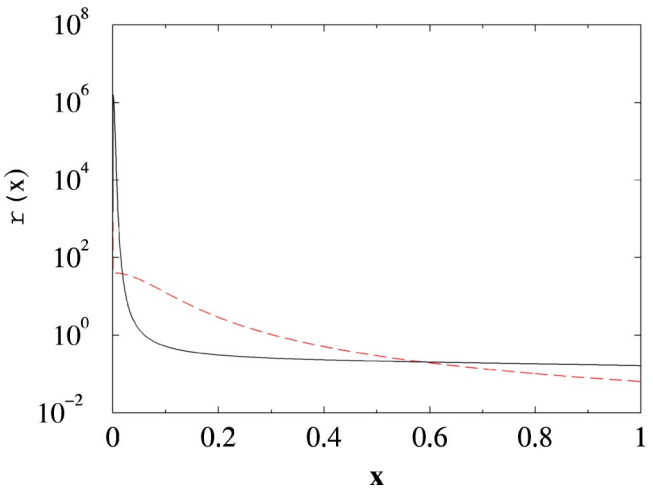

FIG. 2. MF density profiles $\rho_u(x)$ of a uniform state (dashed line) and $\rho_{c-h}(x)$ of a core-halo state (solid line) for $\epsilon=\epsilon_{coll}$.

$$F[\rho(.),\mathbf{x}]=\exp\left[\beta\int\frac{\rho(\mathbf{x}')}{\sqrt{(\mathbf{x}-\mathbf{x}')^2+x_0^2}}d^3\mathbf{x}'\right],$$

$$\beta=\frac{3}{2}\left[\epsilon+\frac{1}{2}\int\int\frac{\rho(\mathbf{x}_1)\rho(\mathbf{x}_2)}{\sqrt{(\mathbf{x}_1-\mathbf{x}_2)^2+x_0^2}}d^3\mathbf{x}_1 d^3\mathbf{x}_2\right]^{-1},$$

$$\rho_0=\left\{\int F[\rho(.),\mathbf{x}]d^3\mathbf{x}\right\}^{-1}. \tag{3}$$

This equation replaces the Poisson-Boltzmann differential equation for the self-consistent potential (see, for example, Ref. [1]), since the interparticle interaction considered here is not purely Coulombic. The equilibrium density profile $\rho(x)$ obtained from this equation is then used to calculate entropy and pressure.

The MF phase diagram of the system is presented in Fig. 1. The collapse and explosion energies are $\epsilon_{coll}\approx-0.339$ and $\epsilon_{expl}\approx0.267$. Examples of the uniform and the core-halo density profiles for $\epsilon=\epsilon_{coll}$ are shown in Fig. 2.

In the MD simulations we consider systems consisting of $N=125$–500 particles in a spherical container of radius $R=1$. All interparticle forces are calculated directly at each time step dt. This is done in order to avoid any mean-field-like effects inevitably present in any truncated multipole or Fourier potential expansion. The particle velocities and coordinates are updated according to the standard velocity Verlet algorithm which is symplectic and time reversible [and correct up to including $O(dt^3)$], as can be shown by a straightforward application of the Trotter expansion [17].

Systems were initialized by randomly distributing particles according to a spherically symmetric density profile. Typically the appropriate MF density profile $\rho(x)$ was used. The potential energy U of the initial configuration was calculated and the target kinetic energy $E_k=E-U$ was determined. The particle velocities were randomly generated from a distribution (usually Maxwell) with the appropriate square average. Finally, the deviation of the total energy from its target value, caused by stochasticity in velocity assignment, was determined and the velocities were rescaled to fine-tune the total energy. Due to the isotropicity of velocity assignment, we always obtained states with sufficiently low total angular momentum which collapsed to single-core states rather than to binaries [10].

To implement reflective boundary conditions, at each time step the normal components $v_\perp$ of the velocities of all particles which had escaped from the container were reversed. Values of the normal components were stored to evaluate the pressure on the wall, i.e.,

$$P(t)=\frac{\sum_{t'=t-t''/2}^{t'=t+t''/2}v_\perp(t')}{2\pi R^2 t''}. \tag{4}$$

During each simulation run we measured the following quantities: kinetic energy $\epsilon_{kin}=3/2\beta$, the virial variable σ quantifying deviations from the virial theorem, $\sigma\equiv\epsilon+\epsilon_{kin}-3PVR/N^2$ [where P is the pressure on the wall, $V=4\pi R^3/3$ is volume of the container, and the factor N^2/R rescales the volume-pressure term to the unit of energy introduced in Eq. (2)], ratio of the velocity moments, $19\langle v^2\rangle^2/5\langle v^4\rangle$ (which should be 1 for the Maxwell distribution), and the number of particles in the core, N_c, of the prescribed radius x_c. For the last measurement we count the number of particles, N_i, that are within x_c from the ith particle and find the particle which has the largest N_i.

In addition, we measured the histograms of the velocity distribution and radial distribution functions $W(u)$ and $C(x)$, respectively. The latter was defined as the number of particles in a spherical layer of radius x around each particle normalized by the volume of the layer and disregarding nonuniformity of the system and boundary effects.

The measurements of scalar quantities such as energy, kinetic energy, pressure, and velocity distribution moments were taken in time intervals τ_{meas}. We usually chose τ_{meas} to be of the order of the crossing time. The histogram data, such as the velocity and radial distribution functions, was incremented at each τ_{meas} and accumulated over a longer time period $\tau_{hist}\sim(10$–$10^3)\tau_{meas}$.

Our attempts to resolve the high-density part of the radial density profile of the system turned out to be fruitless due to the strong fluctuations in its position. These fluctuations smear the central peak in both core-halo and low-energy uniform states. Considering the center of mass system of reference does not resolve this difficulty as, despite being dense, the core typically contains only 10–20 % of the total mass of the system (see below), and the positions of the core and the center of mass of the system do not usually coincide.

To control the quality of simulations, we monitored the total energy ϵ and the total angular momentum L. The time step dt was chosen to be small enough in order to keep the total energy variation within 0.05% of its initial value. Typically we used $dt=10^{-5}$ or $d\tau\sim10^{-4}$ in rescaled units. For such time steps, the relative deviation of the angular momentum was within 10^{-14}.

All the measurements below are presented in the rescaled dimensionless units as defined in Eq. (2).

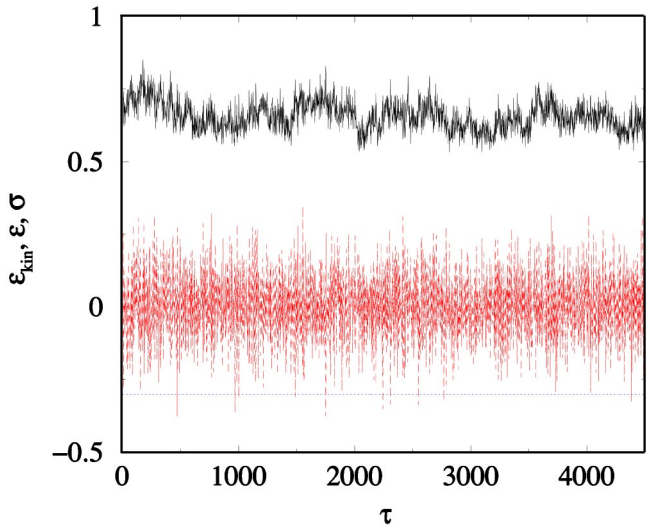

FIG. 3. Plots of time dependence of kinetic energy e_{kin} (solid line), virial variable σ (dashed line), and total energy ϵ (dotted line) for a uniform system of $N=250$ particles at $\epsilon=-0.3$.

III. UNIFORM AND CORE-HALO EQUILIBRIUM STATES: COMPARISON TO MEAN-FIELD THEORY

To check our simulation procedure and to attempt to resolve the apparent contradiction between the MF and the particle simulation results [12], we first considered a system which we expected to be in a stable or a metastable state far away from any transition point. Since we are interested in the equilibrium properties, we initiated the MD simulations according to the corresponding MF predictions, i.e., the density profiles were initialized using the MF profiles and the initial velocities were assigned according to the Maxwell distribution. We observed that initializing the density profiles this way virtually eliminated the transitory period. The method of velocity assignment turned out to be practically unimportant, provided that the correct value for the total kinetic energy was obtained. For example, for a system initialized with a flat velocity distribution $[W(\mathbf{u})=\text{const}]$, it took about $\tau \sim \tau_r$ to evolve to the Maxwell distribution.

A typical plot of the steady state time dependence of the kinetic energy, virial variable, and the total energy is presented in Fig. 3. Comparison between the MD measurements and the MF results for the uniform and core-halo states is presented in Tables I and II. The comparison reveals a perfect agreement between these two sets of data.

The MF virial variable was calculated using

$$\sigma_{MF}=\epsilon+\epsilon_{kin}[1-8\pi\rho(1)/3], \tag{5}$$

TABLE I. Equilibrium MD and MF results for a uniform state for $\epsilon=-0.3$, $N=250$, and $0\leqslant\tau\leqslant5000$.

	MD	MF
ϵ	$-0.3\pm5\times10^{-7}$	-0.3
ϵ_{kin}	0.66 ± 0.05	0.644
σ	0 ± 0.03	0.012
$19\langle v^2\rangle^2/5\langle v^4\rangle$	1.01 ± 0.04	1

TABLE II. Equilibrium MD and MF results for a core-halo state at $\epsilon=-0.339$, $N=250$, and $0\leqslant\tau\leqslant1500$.

	MD	MF
ϵ	$-0.3392\pm2\times10^{-4}$	-0.339
ϵ_{kin}	2.9 ± 0.1	2.94
σ	-1.5 ± 0.1	-1.46
$19\langle v^2\rangle^2/5\langle v^4\rangle$	0.99 ± 0.03	1
N_{core}	48 ± 2	47.6

where the last term comes from the pressure at the container wall, $P=2\rho(x=1)\epsilon_{kin}/3$. Since the interparticle potential is not purely Coulombic, the virial variable is nonzero. The difference is prominent for the core-halo states in which more particles ''probe'' the short-range part of the potential.

To evaluate the core radius and the number of core particles in a core-halo system, we considered an integrated MF density profile, $f(x)=\int_0^x 4\pi y^2\rho(y)dy$ (see Fig. 4). As it follows from Fig. 4, the MF core-halo state indeed contains a distinct core with a sharp boundary of radius $x_c\approx10^{-2}$ relatively insensitive to the energy in the range we considered ($|\epsilon|<0.5$). Using this MF core radius, we located cores in the MD core-halo systems. The number of core particles in MD systems turned out to follow very closely the MF predictions (see Table II). Using a smaller core radius resulted in a significant reduction in the number of MD core particles. A reasonably small overestimation of the core radius did not affect the results of the MD measurements. We observed that even in a sphere of twice the core radius, the number of particles was only marginally (at most by 8%) larger than in the core.

To check if the system has more than one core, we performed searches for the second-largest core of the same radius x_c. We looked for the largest group of particles which are within x_c from a single particle with none of these particles belonging to the first, i.e, to the largest core. We never observed the second-largest core containing more than two particles. Most of the time no second core was observed.

In Fig. 5 we present the MD velocity distribution functions $W(u)$ for core-halo and uniform states. The measured $W(u)$ confirms the MF prediction for the Maxwellian form.

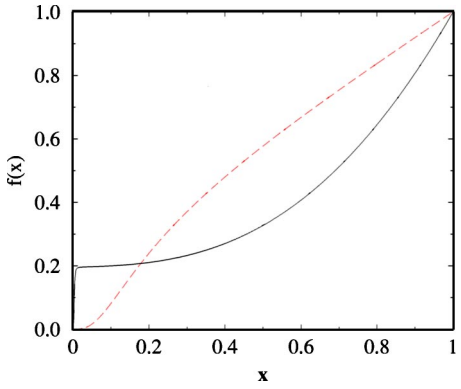

FIG. 4. Integrated MF density profiles $f_u(x)$ of a uniform state (dashed line) and $f_{c-h}(x)$ of a core-halo state (solid line) for $\epsilon=\epsilon_{coll}$.

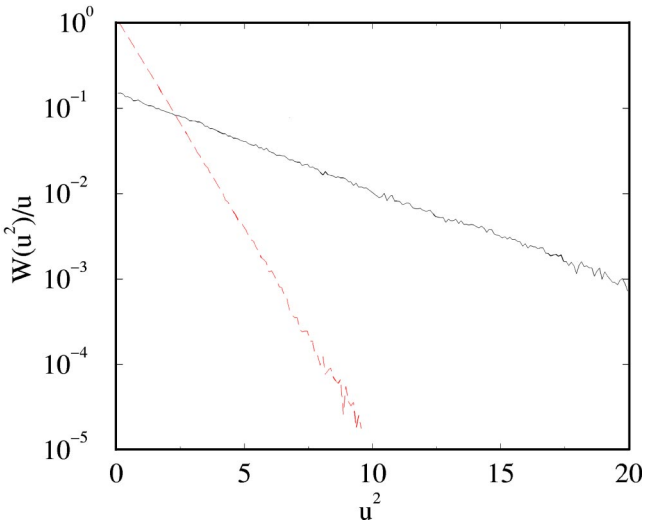

FIG. 5. The MD velocity distribution functions $W(u)$ of a core-halo state with $\epsilon=-0.339$ (solid line) and a uniform state with $\epsilon=-0.3$ (dashed line). In both cases $N=250$.

As we mentioned in the preceding section, we were unable to resolve the high-density part of the radial density profile due to core motion. However, an indirect comparison between the MF and MD radial distributions of particles was made using the radial distribution function. The MF radial distribution function $C_{MF}(x)$ was computed as

$$C_{MF}(x)=\frac{1}{4\pi x^2}\int \rho(\mathbf{x}')\rho(\mathbf{x}+\mathbf{x}')d\mathbf{x}'. \tag{6}$$

The good agreement between the MF and the MD radial distribution functions is illustrated in Fig. 6. This indicates that the mutual distribution of particles is correctly predicted by the MF theory.

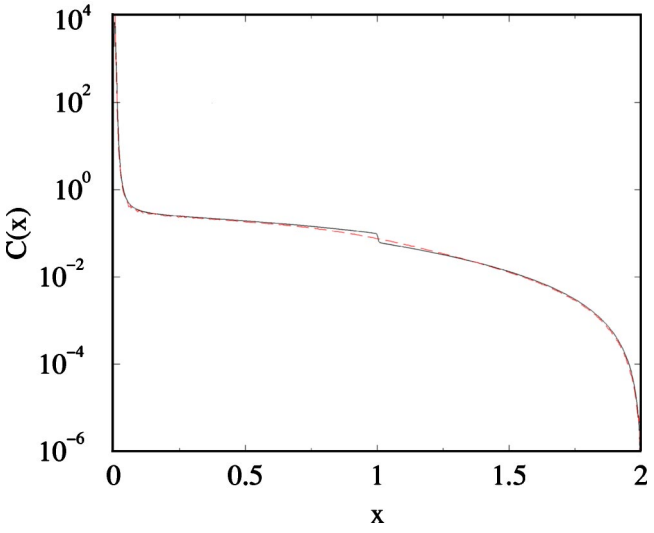

FIG. 6. MF (dashed line) and MD (solid line) radial distribution functions $C(x)$ of a core-halo state with $\epsilon=0.25$. The step at $x=1$ in the MF $C(x)$ is caused by the localization of the core exactly at $x=0$ and a sharp boundary of the container.

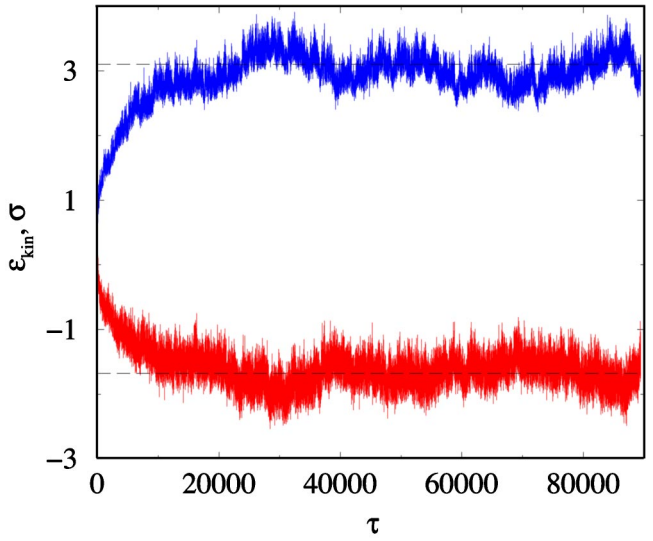

FIG. 7. Time dependence of the kinetic energy ϵ_{kin} (top) and the virial variable σ (bottom) of the collapsing uniform state with $\epsilon=-0.5$ and $N=125$. The dashed horizontal lines indicate the equilibrium values of ϵ_{kin} and σ of the corresponding core-halo state.

To summarize, for all the quantities considered, we observed no systematic deviations between the MF theory and the MD data.

IV. COLLAPSE

The MF theory predicts that if the energy of the uniform state becomes lower than $\epsilon_{coll}\approx-0.339$, the system should undergo a collapse to a core-halo state. To study the collapse, we considered several uniform systems with energies ranging between $\epsilon=-0.5$ and $\epsilon=-0.3$. The systems were initialized according to the MF density distributions. For systems with $\epsilon<\epsilon_{coll}$ the particles were distributed according to the MF density profile for ϵ_{coll}.

In perfect agreement with the MF theory, a uniform state with $\epsilon<\epsilon_{coll}$ undergoes a gradual transition to a core-halo state with a typical time scale of $\tau_{coll}\sim10^4$ for $N=125$–250 particles. An example of the time dependence of the kinetic energy and the virial variable for a collapsing system is shown in Fig. 7. We observe that if the number of particles is increased but the rescaled energy ϵ is kept fixed, it takes generally a longer time (unrescaled time t) for the collapse to be complete. Our results (see Fig. 8) qualitatively confirm that the characteristic time for the full collapse scales as τ_r [16]. However, detailed quantitative study of the dependence of the collapse dynamics on the number of particles requires much faster simulation code.

In the above examples, the energy was set to $\epsilon=-0.5$ which is well below $\epsilon_{coll}\approx-0.339$, and, as a consequence, the collapse started immediately at $\tau=0$ in all simulation runs. If the system energy is ϵ_{coll}, a noticeable increase in the kinetic energy, and a decrease in the virial variable characteristic for a collapse, starts after a small delay (Fig. 9). The delay varies from run to run from almost zero to about

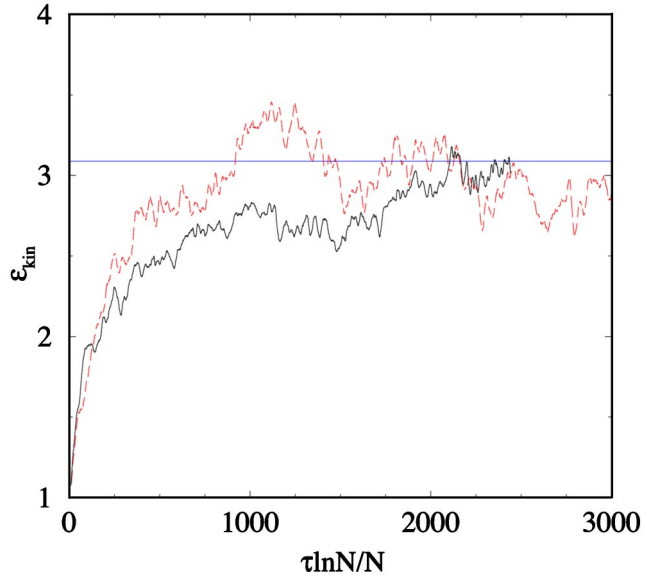

FIG. 8. Collapse in systems with $\epsilon=-0.5$ and different numbers of particles, $N=125$ (dashed line) and $N=250$ (solid line), shown in relaxation time units, $\tau \ln N/N$ [16]. Horizontal line shows the kinetic energy of the target core-halo state. The data is averaged over $\delta\tau=100$ time intervals.

$\tau \approx 1500$. The observed uncertainty is likely to be due to the relatively small number of particles.

As we increase the energy above ϵ_{coll}, the stability of the uniform state increases, leading to a longer lifetime of such a state. Figure 10 displays the evolution of a system at $\epsilon=-0.3$. The system stays in the uniform state for about $\tau \approx 5000$ before the collapse starts, after which the evolution proceeds qualitatively similarly to the collapses in systems with lower energies.

To compare the temporal evolution of the kinetic energy, the virial variable, and the number of core particles, the relative variables $\epsilon'_{kin}(\tau)$, $\sigma'_{kin}(\tau)$, and $N'_{core}(\tau)$ are plotted in Fig. 11. They are defined following $\epsilon'_{kin}(t)=[\epsilon_{kin}(t)-\epsilon_{kin}(u)]/[\epsilon_{kin}(c-h)-\epsilon_{kin}(u)]$. The values $\epsilon_{kin}(u)$ and $\epsilon_{kin}(c-h)$ correspond to the uniform and core-halo states in equilibrium.

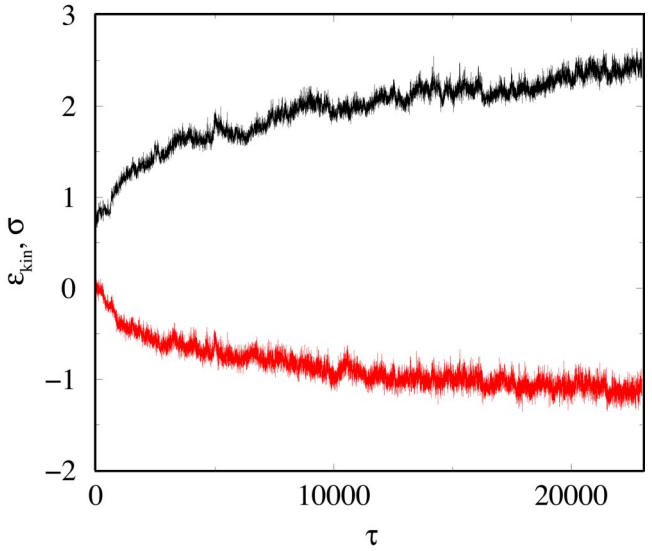

FIG. 9. Plots of the kinetic energy ϵ_{kin} (top) and the virial variable σ (bottom) vs time τ for a system with $\epsilon=\epsilon_{coll}\approx-0.339$ and $N=250$.

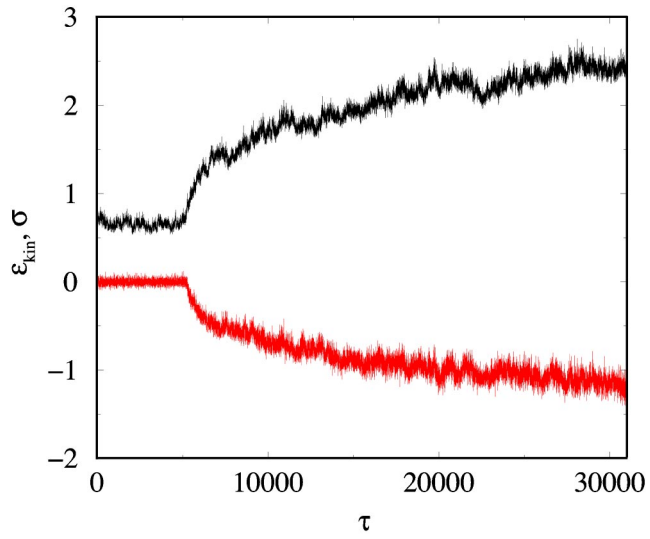

FIG. 10. Plots of the kinetic energy ϵ_{kin} (top) and virial variable σ (bottom) vs time τ for a system with $\epsilon=-0.3$ and $N=250$.

Figure 11 indicates that during the initial stages of a collapse the core evolves faster than the kinetic energy and the virial variable. In addition, one can observe large reversible fluctuations in the number of core particles (the core grows up to 12% of its final value and then disappears) that are not matched by fluctuations of comparable scale in kinetic energy or virial variable. All these observations suggest that the density evolution causing the core formation plays the leading role in the process of collapse while the relaxation of kinetic energy follows. Once the collapse has started, the

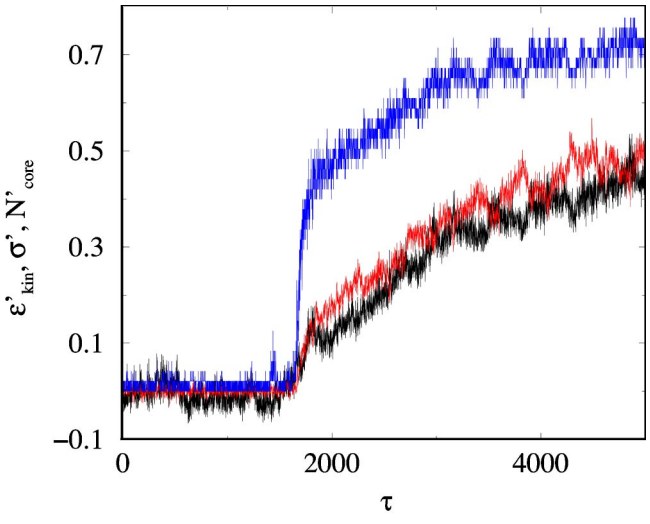

FIG. 11. Plots of the relative values of (from top to the bottom) number of core particles $N'_{core}(\tau)$, virial variable $\sigma'_{kin}(\tau)$, and kinetic energy $\epsilon'_{kin}(\tau)$ for the system with $\epsilon=-0.339$ and $N=250$.

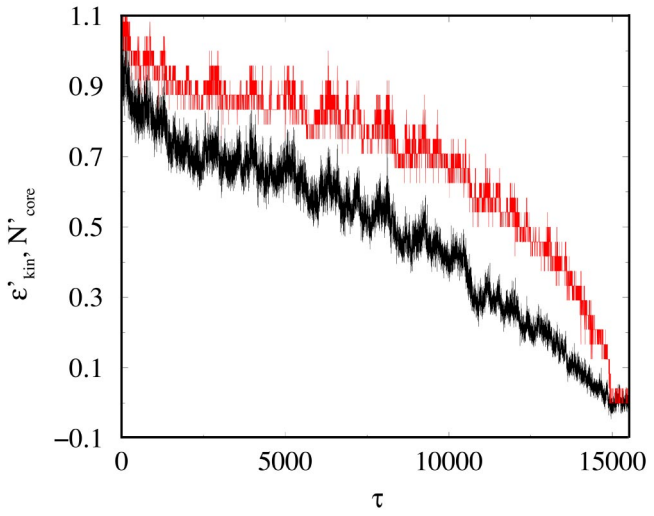

FIG. 12. Plots of the kinetic energy $\epsilon'_{kin}(\tau)$ (top) and relative number of core particles $N'_{core}(\tau)$ (bottom) (defined as in Fig. 11) vs time τ for a system with $\epsilon=0.5$ and $N=250$.

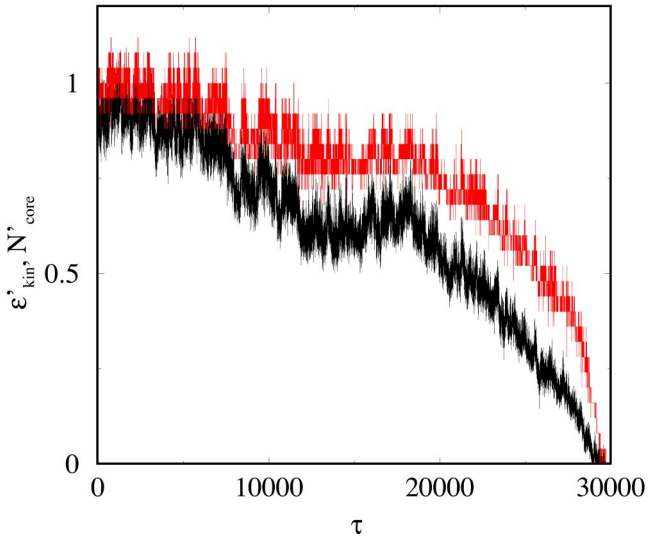

FIG. 13. Same as in Fig. 12 but with $\epsilon=0.4$.

core grows to about half of its final size in only $\tau\sim10^3$ for systems with $N=125$–500 particles. Changes in kinetic energy during this time interval are small. After this rapid initial stage the system relaxes more slowly, and finally after $\tau_{coll}\sim10^5$ reaches the equilibrium core-halo state. Our observations strongly suggest that the growth of the core takes place through a sequential absorption of single particles rather than through a hierarchical merging of smaller cores: We never detected other cores containing more than two particles. Although the kinetic energy relaxation trails behind the core formation, the velocity distribution function remains Maxwellian throughout the whole evolution with the temperature corresponding to the respective value of the kinetic energy. This is caused by the fast velocity relaxation ($\tau_{vel}\sim1$) as discussed in the preceding section.

V. EXPLOSION

It is natural to assume that if a system exhibits a collapse, it should also exhibit an explosion which is the reverse to the collapse transition. According to the MF theory, such an explosion should take place when the core-halo state becomes unstable, i.e., when $\epsilon\geqslant\epsilon_{expl}\approx0.267$. To check this prediction, we initialized the MD system according to the MF equilibrium core-halo state and followed its evolution. As in the study of the collapse, for initial states with $\epsilon>\epsilon_{expl}$ we used the MF density profiles of the (locally) stable state with the highest possible energy, i.e., of the state with $\epsilon=\epsilon_{expl}$.

We observe that a system with sufficiently high energy, such as $\epsilon=0.5$ in Fig. 12 or $\epsilon=0.4$ in Fig. 13, indeed undergoes an explosion which brings it to the uniform equilibrium state. During such an explosion, the state variables such as kinetic energy and the virial variable continuously change from their equilibrium core-halo state values to the uniform state ones, and the core gradually sheds particles until only one particle is left. The main features of an explosion (Figs. 12 and 13) resemble those of a time-reversed collapse. The kinetic energy evolves relatively uniformly, while the number of core particles changes only slightly during the first stages of evolution and rapidly decreases at the final stages. In the example presented in Fig. 12, the explosion is complete after time $\tau_{expl}\approx15\,000$, which is considerably less than the time for a collapse $\tau_{coll}\approx10^5$ (see Fig. 8) in a system having the same number of particles ($N=250$). However, the latter is less precisely defined due to larger fluctuations in a core-halo than in a uniform state.

Similarly to a collapse, the system remains thermalized in the velocity space during an explosion. The velocity distribution remains Maxwellian throughout the evolution with the temperature corresponding to the current value of kinetic energy. As an illustration, Fig. 14 shows the ratio of the Âmoments of the MD velocity distribution, $19\langle v^2\rangle^2/5\langle v^4\rangle$, which should be 1 for a Gaussian distribution.

It is evident from a comparison between Figs. 12 and 13 that as ϵ gets closer to ϵ_{expl} the explosion takes longer to

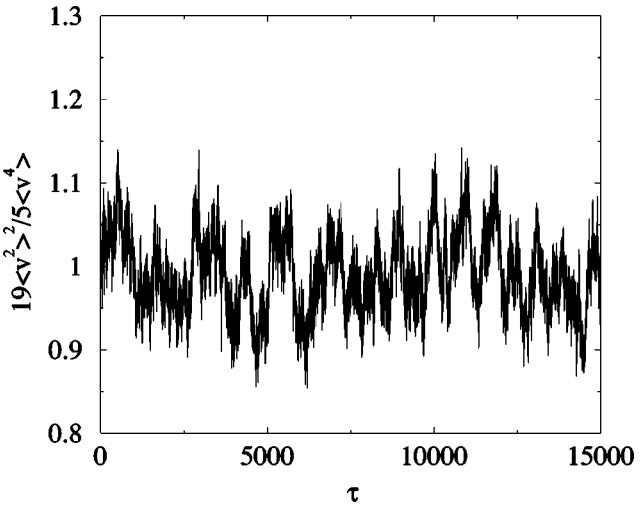

FIG. 14. Plot of the ratio of the moments of velocity distribution, $19\langle v^2\rangle^2/5\langle v^4\rangle$, vs time τ for a system with $\epsilon=0.5$ and $N=250$.

initiate. We have observed that even for $\epsilon = 0.3$, which is noticeably larger than $\epsilon_{expl} \approx 0.267$, the explosion does not occur for $\tau < 30\,000$. This suggests that either the MF value for ϵ_{expl} is incorrect or the initialization does not put the system exactly into equilibrium (metastable) core-halo state. If the latter is the case, deviations from equilibrium would most probably take place in the core. Due to its compactness and strongly correlated nature, its equilibration with the rest of the system may take a rather long time. Using the current MD setup, we were unable to determine the reason for this apparent discrepancy.

VI. CONCLUSIONS

In the previous sections we have presented the following molecular dynamics results for self-attracting systems with soft Coulomb potential.

(1) A collapse from a uniform to a core-halo state was observed. The time scale for the collapse in systems consisting of 125–500 particles is of the order of 10^5 crossing times and is by the same factor longer than the time scale of the velocity relaxation. The collapse starts with a fast growth of a core via absorption of single particles and continues with more gradual relaxation towards an equilibrium core-halo state. Metastable states exhibit finite lifetimes before collapsing.

(2) A reverse to collapse, i.e., an explosion transition from a core-halo to a uniform state was observed. The explosion time is considerably shorter than the collapse time, being of the order of 10^4 crossing times (125–500 particles). An explosion resembles a time-reversed collapse; the core decrease, which proceeds by shedding individual particles, is trailing the kinetic energy evolution until the last stages when the core rapidly disappears.

(3) Molecular dynamics results for the equilibrium and the metastable uniform and core-halo states are found to be equal within statistical uncertainty to the corresponding mean-field predictions. These quantities include kinetic energy, wall pressure, number of core particles, particle-particle radial distribution function, and velocity distribution function.

The long collapse time observed in our simulations appears to be an explanation for the apparent discrepancy between the phase diagram presented in Ref. [12] and the mean-field phase diagram (see, for example, Ref. [9]). The relaxation time allowed for a system to reach a steady state in Ref. [12] was $t_{rel} = 3N/|EN|^{3/2}$, which is apparently equivalent to $\tau_{rel} < 1$ in rescaled units [Eq. (2)]. This is insufficient for a system to collapse. Therefore, discontinuities in caloric curves β vs ϵ, typical for collapse and explosion gravitational transitions, were not observed in Ref. [12].

Although we considered systems only with the soft Coulomb potential, we speculate that a likewise similarity between the mean-field and molecular dynamics equilibrium properties of the core-halo state exists for all ''soft'' long-range (such as a Fourier- or spherical harmonic-truncated Coulomb) potentials. We attribute this to the fact that all soft potentials are effectively longer ranged than the bare Coulomb one. When the interparticle distance becomes small compared to the respective softening radius (given by r_0 or determined by the order of truncation in the expansions mentioned above) all these soft potentials tend to a constant, and the interparticle force vanishes continuously. Another similarity between the soft potentials is that a core radius is independent of the number of core particles, unlike, for example, radius of a core consisting of impenetrable particles of finite radius. The core-halo state in a system with a ''harder'' short-range cutoff may have completely different properties from the one considered above and mean-field theory may become inadequate. As for uniform states, their properties are virtually independent of the nature of the cutoff (see, for example, Ref. [9]) and their mean-field description is universally correct.

The main goal in this paper was to check the existence of collapses and explosions and the validity of the mean-field data for self-gravitating systems with short-range cutoff. For this goal a few molecular dynamics runs for each system were sufficient. However, to be able to study the dynamical features of collapses and explosions in more detail and to compare the simulation results to various theoretical models, one needs to study the relaxation averaged over many initial configurations. For example, an interesting question is whether a collapse (or an explosion) indeed consists of two stages: The first fast stage of collisionless ''violent relaxation'' with particle number-independent rate and the slower second stage of soft collisional relaxation with characteristic time τ_r (see, for example, Ref. [16] and references therein). Another important question is to resolve the apparent contradiction between the mean-field prediction for ϵ_{expl} and the molecular dynamics observations outlined at the end of the preceding section. Such studies require a more efficient simulation code. The main improvement may possibly come from a better force calculator that could include various mean-field-like potential expansions, which are qualitatively justified by this study. We leave this for the future research.

ACKNOWLEDGMENTS

The authors are thankful to P.-H. Chavanis and E. G. D. Cohen for helpful and inspiring discussions and gratefully acknowledge the support of Chilean FONDECYT under Grant Nos. 1020052 and 7020052. M.K. would like to thank the Department of Physics at Universidad de Santiago for warm hospitality.

[1] T. Padmanabhan, Phys. Rep. **188**, 285 (1990).
[2] B. Stahl, M.K.-H. Kiessling, and K. Schindler, Planet. Space Sci. **43**, 271 (1995).
[3] P.-H. Chavanis and J. Sommeria, Mon. Not. R. Astron. Soc. **296**, 569 (1998).
[4] V.P. Youngkins and B.N. Miller, Phys. Rev. E **62**, 4583 (2000).
[5] I. Ispolatov and E.G.D. Cohen, Phys. Rev. E **64**, 056103 (2001), Phys. Rev. Lett. **87**, 210601 (2001).
[6] H.J. de Vega and N. Sánchez, Nucl. Phys. B **625**, 409 (2002).
[7] P.H. Chavanis, Phys. Rev. E **65**, 056123 (2002).

[8] P.H. Chavanis, C. Rosier, and C. Sire, Phys. Rev. E **66**, 036105 (2002).
[9] P.H. Chavanis and I. Ispolatov, Phys. Rev. E **66**, 036109 (2002).
[10] E.V. Votyakov, H.I. Hidmi, A. De Martino, and D.H.E. Gross, Phys. Rev. Lett. **89**, 031101 (2002).
[11] P.H. Chavanis and M. Rieutord, e-print astro-ph/0302594.
[12] M. Cerruti-Sola, P. Cipriani, and M. Pettini, Mon. Not. R. Astron. Soc. **328**, 339 (2001).
[13] C. Lancellotti and M. Kiessling, Astrophys. J. **549**, L93 (2001).
[14] P. Hut, M.M. Shara, S.J. Aarseth, R.S. Klessen, J.C. Lombardi, Jr., J. Makino, S. McMillan, O.R. Pols, P.J. Teuben, and R.F. Webbink, New Astron. **8**, 337 (2003).
[15] J. Katz and I. Okamoto, Mon. Not. R. Astron. Soc. **317**, 163 (2000).
[16] J. Binney and S. Tremaine, *Galactic Dynamics*, Princeton Series in Astrophysics (Princeton University Press, Princeton, NJ, 1988).
[17] M. Tuckerman, B.J. Berne, and G.J. Martyna, J. Chem. Phys. **97**, 1990 (1992).